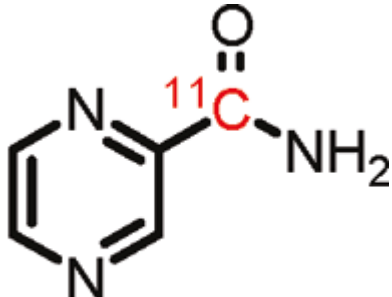


^{11}C -Labeled pyrazinamide [^{11}C]PZA

Liang Shan, PhD^{✉1}

Created: August 2, 2010; Updated: October 1, 2010.

Chemical name:	^{11}C -Labeled pyrazinamide	
Abbreviated name:	[^{11}C]PZA	
Synonym:		
Agent Category:	Compounds	
Target:	Type 1 fatty acid synthases	
Target Category:	Enzymes (bacteria)	
Method of detection:	Positron emission tomography (PET)	
Source of signal / contrast:	^{11}C	
Activation:	No	Structure of [^{11}C]PZA by Liu et al (1). Click on the PubChem for additional information about PZA.
Studies:	<ul style="list-style-type: none"> <i>In vitro</i> Non-human primates 	

Background

[[PubMed](#)]

Pyrazinamide (PZA) is a prodrug used in the treatment of *Mycobacterium tuberculosis* (MTB) infection. PZA is converted to its active form, pyrazinoic acid, by the pyrazinamidase of MTB at the acidic site of infection. Pyrazinoic acid inhibits the type 1 fatty acid synthases of the bacilli. Accumulation of pyrazinoic acid is also thought to disrupt the membrane potential and interfere with the energy production necessary for survival of MTB. Mutations of the pyrazinamidase gene are responsible for the development of PZA resistance. PZA is largely bacteriostatic. PZA labeled with ^{11}C ([^{11}C]PZA) has been generated by Liu et al. for *in vivo* and real-time analysis of the PZA pharmacokinetics (PK) and biodistribution with positron emission tomography (PET) (1). The half-life of ^{11}C is 20.4 min.

The PK and biodistribution of a novel drug are traditionally determined with blood and tissue sampling and/or autoradiography. Despite high workload and huge investment in drug development, only 8% of the drugs entering clinical trials today reach the market, as estimated by the U.S. [Food and Drug Administration](#). One main reason for this attrition is insufficient exploration of the *in vivo* drug–target interaction (1). Traditional methods are inadequate to answer questions such as whether a drug reaches the target, how the drug interacts with its targets, and how the drug modifies the diseases. Because of the high resolution and sensitivity of newly developed imaging techniques, investigators have become increasingly interested in addressing these issues (2, 3). In the case of PET imaging, most small molecules can now be efficiently labeled with ^{11}C or with ^{18}F at $>37\text{ GBq}/\mu\text{mol}$ ($1\text{ Ci}/\mu\text{mol}$), and they can be detected with PET in the nanomolar to picomolar concentration range (4–6). Consequently, a sufficient signal for imaging can be obtained even though the total amount of a radiotracer administered systemically is extremely low (known as microdosing, typically $<1\text{ }\mu\text{g}$ for humans). Microdosing is particularly valuable for evaluating tissue exposure in the early phase of drug development when the full-range toxicology is not yet available (7, 8). Increasing evidence has demonstrated the efficiency of PET imaging in obtaining quantitative information on drug PK and distribution in various tissues including brain; confirming drug binding with targets and elucidating the relationship between occupancy and target expression/function *in vivo*; assessing drug passage across the blood–brain barrier (BBB) and ensuring sufficient exposure to brain for central nervous system drugs; and dissecting the modifying effects of drugs on diseases (2, 4, 5).

The current treatment regime for drug-sensitive TB involves the use of rifampicin (RIF), isoniazid (INH), PZA, and ethambutol or streptomycin for two months, followed by four months of continued dosing with INH and RIF (9, 10). This regime is primarily based on PK studies in serum and on efficacy of treatment. The efficacy of each drug for different types of TB such as brain TB and the drug distribution in each compartment of an organ are not well understood. To provide direct insights into these drugs, Liu et al. labeled INH, RIF, and PZA with ^{11}C and used PET to investigate their PK and biodistribution in baboons (1). Liu et al. found that the organ distribution and BBB penetration of each drug differed greatly. $[^{11}\text{C}]\text{PZA}$ can easily penetrate the BBB ($\text{PZA} > \text{INH} > \text{RIF}$); however, the PZA concentrations in the cerebrospinal fluid and brain were only slightly higher than its minimum inhibitory concentration (MIC) value against TB. This chapter summarizes the data obtained by Liu et al. regarding $[^{11}\text{C}]\text{PZA}$. The data obtained with regard to $[^{11}\text{C}]\text{RIF}$ and $[^{11}\text{C}]\text{INH}$ are described in the MICAD chapters on $[^{11}\text{C}]\text{RIF}$ and $[^{11}\text{C}]\text{INH}$, respectively.

Related Resource Links:

- [Challenge and Opportunity on the Critical Path to New Medical Products, FDA](#)
- [PZA compounds in PubChem Substance](#)
- [Clinical trials for diagnosis and treatment of tuberculosis in ClinicalTrials.gov](#)
- MICAD chapters on $[^{11}\text{C}]\text{RIF}$ and $[^{11}\text{C}]\text{INH}$

Synthesis

[PubMed]

Liu et al. synthesized $[^{11}\text{C}]\text{PZA}$ in two steps, starting with $[^{11}\text{C}]\text{HCN}$. Initially, $[^{11}\text{C}]\text{cyanopyrazine}$ was generated with a 90% radiochemical yield in a 5-min reaction of 2-iodopyrazine and $[^{11}\text{C}]\text{HCN}$ with tetrakis(triphenylphosphine)palladium as the catalyst. Subsequent hydrolysis of the cyano group was accomplished in an additional 5 min by treating $[^{11}\text{C}]\text{cyanopyrazine}$ with hydrogen peroxide under basic conditions. The overall decay-corrected yield was 50%–55% (calculated from $[^{11}\text{C}]\text{HCN}$) with a total synthesis time of 45 min. The final product was $>99\%$ radiochemically pure with a specific activity of 4.44–5.55 $\text{GBq}/\mu\text{mol}$ (120–150 $\text{mCi}/\mu\text{mol}$).

In Vitro Studies: Testing in Cells and Tissues

[PubMed]

The lipophilicity (logD) of [¹¹C]PZA was measured on the basis of octanol–water partitioning. The plasma protein binding (% of free fraction in plasma) of [¹¹C]PZA was determined after incubation with baboon plasma for 10 min at room temperature. The results showed that the logD was –0.41 and the plasma protein binding was 91.32%, which are similar to literature values reported elsewhere (1).

Animal Studies

Rodents

[PubMed]

No references are currently available.

Other Non-Primate Mammals

[PubMed]

No references are currently available.

Non-Human Primates

[PubMed]

Liu et al. used PET imaging to study the biodistribution of [¹¹C]PZA in healthy baboons ($n = 4$) (1). The PZA concentrations in the brain and other organs were estimated on the basis of the weight of the baboon, a standard daily dose (20 mg/kg for a human adult), and the assumption that the positron signal derives primarily from the intact drug.

PZA exhibited excellent penetration into the brain tissue (PZA > INH > RIF). Similar to RIF and INH, PZA showed a higher concentration in the brain tissue than in the CSF, and both concentrations were higher than observed in the serum. For example, at 60 min after injection, the PZA concentration in the brain was 0.00463% injected dose per cubic centimeter (ID/cc), while the PZA concentration was 0.00272% ID/cc in the plasma. In the brain tissue, the PZA concentration exhibited a gradual decrease after injection with 0.00619% ID/cc (21.05 µg/ml) at 30 min, 0.00463% ID/cc (15.74 µg/ml) at 60 min, and 0.00403% ID/cc (13.70 µg/ml) at 90 min after injection. The concentrations at all time points were similar to or only slightly greater than the MIC value for this drug against MTB.

The detailed data about the [¹¹C]PZA distribution in other organs were presented in table 4 in the paper published by Liu et al (1). In general, the calculated PZA concentration was one to three times higher than the MIC of this compound against MTB. [¹¹C]PZA and/or its radiolabeled metabolites rapidly penetrated the heart, lungs, liver, and kidneys, and the tissue concentration of PZA exceeded the concentration in serum in all cases with the exception of the kidney cortex. Similar to the findings with RIF and INH, the differences of PZA concentrations in organs among different species in the literature reports were explained by the interspecies variation and radionuclide difference (1).

Human Studies

[PubMed]

No references are currently available.

References

1. Liu L., Xu Y., Shea C., Fowler J.S., Hooker J.M., Tonge P.J. *Radiosynthesis and bioimaging of the tuberculosis chemotherapeutics isoniazid, rifampicin and pyrazinamide in baboons.* . J Med Chem. 2010;53(7):2882–91. PubMed PMID: 20205479.
2. Fox G.B., Chin C.L., Luo F., Day M., Cox B.F. *Translational neuroimaging of the CNS: novel pathways to drug development.* . Mol Interv. 2009;9(6):302–13. PubMed PMID: 20048136.
3. Komoda F., Suzuki A., Yanagisawa K., Inoue T. *Bibliometric study of radiation application on microdose useful for new drug development.* . Ann Nucl Med. 2009;23(10):829–41. PubMed PMID: 19862482.
4. Hammond L.A., Denis L., Salman U., Jerabek P., Thomas C.R. Jr, Kuhn J.G. *Positron emission tomography (PET): expanding the horizons of oncology drug development.* . Invest New Drugs. 2003;21(3):309–40. PubMed PMID: 14578681.
5. Lancelot, S. and L. Zimmer, *Small-animal positron emission tomography as a tool for neuropharmacology.* Trends Pharmacol Sci, 2010
6. Lee C.M., Farde L. *Using positron emission tomography to facilitate CNS drug development.* . Trends Pharmacol Sci. 2006;27(6):310–6. PubMed PMID: 16678917.
7. Bauer M., Wagner C.C., Langer O. *Microdosing studies in humans: the role of positron emission tomography.* . Drugs R D. 2008;9(2):73–81. PubMed PMID: 18298126.
8. Wagner C.C., Muller M., Lappin G., Langer O. *Positron emission tomography for use in microdosing studies.* . Curr Opin Drug Discov Devel. 2008;11(1):104–10. PubMed PMID: 18175273.
9. Tomioka H. *Current status of some antituberculosis drugs and the development of new antituberculous agents with special reference to their in vitro and in vivo antimicrobial activities.* . Curr Pharm Des. 2006;12(31):4047–70. PubMed PMID: 17100611.
10. Aristoff P.A., Garcia G.A., Kirchhoff P.D., Hollis Showalter H.D. *Rifamycins--obstacles and opportunities.* . Tuberculosis (Edinb). 2010;90(2):94–118. PubMed PMID: 20236863.